

Uremia Accelerates both Atherosclerosis and Arterial Calcification in Apolipoprotein E Knockout Mice

Ziad A. Massy,^{*§} Ognjen Ivanovski,^{*} Thao Nguyen-Khoa,^{*†} Jesus Angulo,[‡] Dorota Szumilak,^{*} Nadya Mothu,^{*} Olivier Phan,^{*} Michel Daudon,[†] Bernard Lacour,[†] Tilman B. Drüeke,^{*} and Martin S. Muntzel^{||}

^{*}INSERM Unit 507 and [†]Laboratory of Biochemistry A, Necker Hospital, Paris, and [‡]Centre de Morphologie Mathématique, Ecole des Mines, Fontainebleau, France; and [§]Divisions of Clinical Pharmacology and Nephrology, University of Picardie and Amiens University Hospital, Amiens; and ^{||}Department of Biological Sciences, Lehman College, Bronx, New York

Chronic renal failure (CRF) favors the development of atherosclerosis and excessive calcification of atheromatous lesions. CRF was induced in apolipoprotein E knockout (apoE^{-/-}) mice to study (1) a possible acceleration of aortic atherosclerosis, (2) the degree and type of vascular calcification, and (3) factors involved in the calcification process. For creating CRF, 8-wk-old apolipoprotein E gene knockout (apoE^{-/-}) mice underwent partial kidney ablation. Control animals underwent sham operation. Aortic atherosclerotic plaques and calcification were evaluated using quantitative morphologic image processing. At 6 wk after nephrectomy, CRF mice had significantly higher serum urea, cholesterol, and triglyceride concentrations than non-CRF controls. The serum levels of advanced oxidation protein products were elevated in the uremic group and were correlated with serum urea levels. Atherosclerotic lesions in thoracic aorta were significantly larger in uremic apoE^{-/-} mice than in nonuremic controls. The relative proportion of calcified area to total surface area of both atherosclerotic lesions and lesion-free vascular tissue was increased in aortic root of uremic apoE^{-/-} mice when compared with controls. The calcium deposits were made of hydroxyapatite and calcite crystals. In addition, plaques from uremic animals showed a significant increase in collagen content, whereas the degree of macrophage infiltration was comparable in both groups. There was no difference in mean arterial BP. These findings demonstrate that CRF aggravates atherosclerosis in apoE^{-/-} mice. Moreover, CRF enhances arterial calcification at both atheromatous intimal sites and atheroma-free medial sites. We anticipate that this experimental model will be useful to test treatment strategies aimed at decreasing the accelerated atherosclerosis and arterial calcification in uremia

J Am Soc Nephrol 16: 109–116, 2005. doi: 10.1681/ASN.2004060495

Accelerated atherosclerosis is one of the primary causes of morbidity and mortality in patients with chronic renal failure (CRF) (1,2). A high frequency of vascular lesions and events has been documented by retrospective studies and more convincingly by prospective analyses (3–6). Although classic risk factors such as advanced age, hypertension, glucose intolerance, and dyslipidemia are important in these patients, hyperphosphatemia, hypercalcemia, and/or an elevated calcium × phosphate product may play a predominant role by favoring both arterial and cardiac valve calcification and cardiovascular mortality.

In recent years, growing interest has been devoted to arterial calcification in CRF patients. Both the intima and media arterial layers are more frequently and more intensively calcified in

uremic patients than in nonuremic individuals, and vascular and valvular calcification is a predictor of increased cardiovascular mortality and morbidity (7–9). In the atheromatous plaque, the most marked difference between uremic and nonuremic patients is not in its size but its composition, with a marked increase in calcium content (10,11). There are also major differences in vessel wall function in relation to media calcification, as reflected by arterial stiffening, which accounts for reduced vascular distensibility and increased vascular resistance in CRF patients (12).

It is important to identify therapeutic means to counteract or even prevent the progression of atheromatous vessel lesions and vascular calcification in CRF patients and thereby to decrease the high incidence of cardiovascular events and mortality. With this in mind, we have been involved in the creation of new experimental models to gain better insight into the mechanisms underlying the accelerated atherosclerosis and arterial calcification of CRF patients and to test possible new therapeutic strategies. However, uremic rats or mice do not easily develop atheromatous lesions. We (13) and others (14,15) reasoned that the apolipoprotein E gene knockout (apoE^{-/-}) mouse may constitute a suitable model to address this issue.

Received June 24, 2004. Accepted October 13, 2004.

Published online ahead of print. Publication date available at www.jasn.org.

Address correspondence to: Dr. Ziad A. Massy, INSERM Unit 507, Necker Hospital, 161, Rue de Sèvres 75015 Paris, France. Phone: + 33-1-44-49-52-34; Fax: + 33-1-45-66-51-33; E-mail: massy@u-picardie.fr

Drs. Ziad A. Massy and Ognjen Ivanovski contributed equally to this article.

ApoE^{-/-} mice have delayed clearance of lipoproteins, and when placed on low-cholesterol, low-fat diets, their total serum cholesterol levels reach 11 to 13 mM as a result of the accumulation of chylomicrons and cholesterol-rich VLDL remnants, as compared with 2 to 3 mM in wild-type mice. Importantly, they develop not only fatty streaks but also widespread fibrous plaques at vascular sites that are typically affected in human atherosclerosis (16). The aim of the present study was to develop an experimental model of accelerated atherosclerosis and vascular calcification in apoE^{-/-} mice with superimposed CRF.

Materials and Methods

Animals

All experiments were performed in apoE^{-/-} mice, which were obtained from IFFA-Credo (Lyon, France) and bred at the Necker Medical Faculty (Paris, France). The mice were housed in polycarbonate cages in a pathogen-free facility set on a 12-h light-dark cycle and given free access to water and regular laboratory chow (Harlan Teklad Global Diets). The components of the diet as listed by the manufacturer were 5.7% fat, 18.9% protein, 72.3% carbohydrates, 1.01% calcium, 0.65% phosphorus, 0.2% magnesium, and 1540 IU/kg vitamin D₃. All procedures were in accordance with National Institutes of Health guidelines for the care and use of experimental animals (NIH publication No. 85-23). After sexual maturation at 4 wk of age, the mice were separated by sex and housed in groups of up to five.

Creation of CRF

At 8 wk of age, the animals were randomly assigned into a uremic group (14 female, 8 male mice) and a nonuremic control group (19 female, 6 male mice). We used a two-step procedure to create uremia. Briefly, we applied cortical electrocautery to the right kidney through a 2-cm flank incision and performed left total nephrectomy through a similar incision 2 wk later as described by Gagnon *et al.* (17). In an initial series aimed at inducing severe reductions in renal function, we observed a 100% mortality of apoE^{-/-} mice at 24 h after contralateral kidney ablation, although 12 of 16 C57BL/6J mice survived for several weeks after the same degree of renal mass reduction (unpublished personal observations). Because the intensity of electrocoagulation determines the degree of CRF, we then aimed to produce a more moderate reduction in renal function and obtained serum urea concentrations between 25 and 30 mM. Control animals received sham operation that included decapsulation of both kidneys. Special care was taken to avoid damage to the adrenals. At 6 wk after surgery, mice were killed by exsanguination under ketamine/xylazine anesthesia (100 mg/kg and 20 mg/kg) in the nonfasting state.

Biochemical Serum Determinations

Blood was collected from the abdominal aorta into chilled dry tubes and spun in a refrigerated centrifuge, and serum was stored at -80°C. Serum levels of urea, total cholesterol, and triglycerides were assessed using a Hitachi 917 autoanalyzer (Roche, Meylan, France). Serum levels of advanced oxidation protein products (AOPP) were measured by spectrophotometry with a microplate reader as described previously (18). In separate groups of male and female apoE^{-/-} mice (18 uremic mice and 24 control mice), we measured serum calcium and phosphorus with a Hitachi 917 autoanalyzer and mouse intact parathyroid hormone (iPTH) using a two-site ELISA (Immutopics, Quidel, France).

Quantification of Atheromatous Lesions in Aorta

For the aortic root sections, the vasculature was perfused with sterile PBS, and the ventricular edge and approximately 1 mm of the aortic root were immediately dissected under a microscope and cryomounted in optimal cutting temperature embedding medium. Cryosections, cut in 10- μ m-thick slices, were collected and numbered from the appearance of the first cusp (point 0). Sections at 200-, 400-, 600-, and 800- μ m distances from the cusps were stained with oil red-O, counterstained with hematoxylin, and mounted under coverslips. For the thoracic aorta sections, the vasculature was perfused and aortic sections from the left subclavian artery to the last intercostal artery branch were dissected and cryomounted. Cryosections, cut in 10- μ m thicknesses, were numbered beginning at 4 mm distal from the left subclavian artery (point 0). Sections at 100-, 200-, 300-, and 400- μ m distances from point 0 were stained as described above. The stained cryosections were magnified at $\times 5$, and the images were captured on a microcomputer equipped with a program developed in Quips language that permitted quantification of the lesions (Leica, Cambridge, UK). The cross-section surface area of the vessel and cross-section surface area of the lesion were assessed.

Quantitative and Qualitative Evaluation of Aorta Calcification

Vascular calcifications in aortic root were evaluated by von Kossa staining in cryosections of aortic tissue. Briefly, the cryosections were placed in 5% silver nitrate solution (Sigma Aldrich, St. Louis, MO) for 30 min in darkness. Then, they were put in revelator solution (Kodak) for 5 min and fixed in 5% sodium-thiosulfate solution for another 5 min. Finally, they were stained with 2% eosin. Calcium deposits appeared in black on a bright red-colored surrounding tissue. We developed morphologic image processing algorithms for computer-assisted automated quantitative measurement of calcification from aortic sections (19), revealed from the von Kossa's silver nitrate staining. Calcium deposits were measured inside and outside atherosclerotic lesions, reflecting atherosclerotic and medial calcium deposits, respectively. Data were expressed as the relative proportion of calcified area to total surface area of either the inside or the outside of atherosclerotic lesions and as the size of calcification granules on either surface, as described previously (19).

To perform additional qualitative characterization of vascular calcification type in CRF apoE^{-/-} mice, we performed Fourier transform infrared (FTIR) spectroscopy of the vascular tissue (Bruker vector 22, Bruker A590 microscope) (20).

Quantification of Monocyte-Macrophage Infiltration and Collagen Content in Aortic Lesions

Monocyte-macrophages (MOMA) were detected in atherosclerotic lesion by immunostaining as described previously (21). Briefly, aortic sections were incubated with 10% normal goat serum for 30 min at room temperature, washed in PBS, and incubated with a primary rat monoclonal antibody against mouse macrophages (clone MOMA-2; BioSource International, Camarillo, CA) for 1 h at room temperature. The secondary antibody was a biotin-horseradish peroxidase-conjugated goat anti-rat IgG (Vector Laboratories, Biovalley, Marne la Vallée, France). Immunostainings were visualized after incubation with a peroxidase detection system (Vectastain ABC kit, Vector Laboratories) using 3-amino 9-ethyl carbazole (Sigma Aldrich) as substrate. At least four sections per animal were analyzed for each immunostaining.

The lesion collagen content was determined by staining with Sirius red (21). The image was captured on a microcomputer equipped with Histolab software (Microvision Instruments, Envy, France) and ana-

lyzed by computerized image analysis measuring the relative area/density in 12 continuous fields in each Sirius red–stained section. Because collagen content may depend on the size of the lesions, only large lesions were examined for determination of content.

BP Measurements

In a separate set of CRF apoE^{-/-} mice (3 female, 3 male mice) and age-matched nonuremic apoE^{-/-} control mice (3 female, 3 male mice), we measured mean arterial BP at the day of killing using direct intra-arterial recording as described previously (22). Briefly, the mice were anesthetized with ketamine/xylazine (100 mg/kg and 20 mg/kg, intraperitoneally), and a PE50 catheter, stretched to reduce the tip diameter, was inserted into the abdominal aorta. The catheter was filled with heparinized saline (20 U/ml), and the distal end was attached to a BP transducer (Gould pressure processor). After a 5-min stabilization period, three BP tracings were obtained, and BP was averaged from the three measurements.

Statistical Analyses

Data were analyzed by ANOVA, linear regression analyses, and unpaired *t* test, as appropriate. Results were expressed as means ± SEM. Differences between groups were considered significant at *P* < 0.05.

Results

Body Weight and Serum Biochemistry

Body weight did not differ between the uremic and nonuremic apoE^{-/-} mice throughout the study (24.4 ± 1.3 versus 23.5 ± 1.2 g, respectively). Serum urea levels were used to assess renal function. At 6 wk after surgery, serum urea concentrations in CRF mice increased by 225% above baseline and tended to be stable, with minimal variations during the 6-wk period (Figure 1A). Serum total cholesterol and triglyceride concentrations were significantly higher in CRF mice compared with non-CRF controls (Figure 1, B and C). Serum AOPP levels were significantly higher in CRF animals than in controls (Figure 1D). By linear regression analysis, AOPP values were closely associated with serum urea values (*r*² = 0.71, *P* < 0.001; Figure 2).

Uremic animals had higher serum calcium and phosphate concentrations (*P* < 0.001, *P* < 0.05, respectively; Table 1) and higher serum iPTH values (*P* < 0.05; Table 1). Mean arterial BP was comparable between the groups (Table 1).

Atheromatous Lesions of Aorta

Six weeks of CRF significantly increased aortic plaque area fraction in thoracic aorta in CRF mice compared with controls

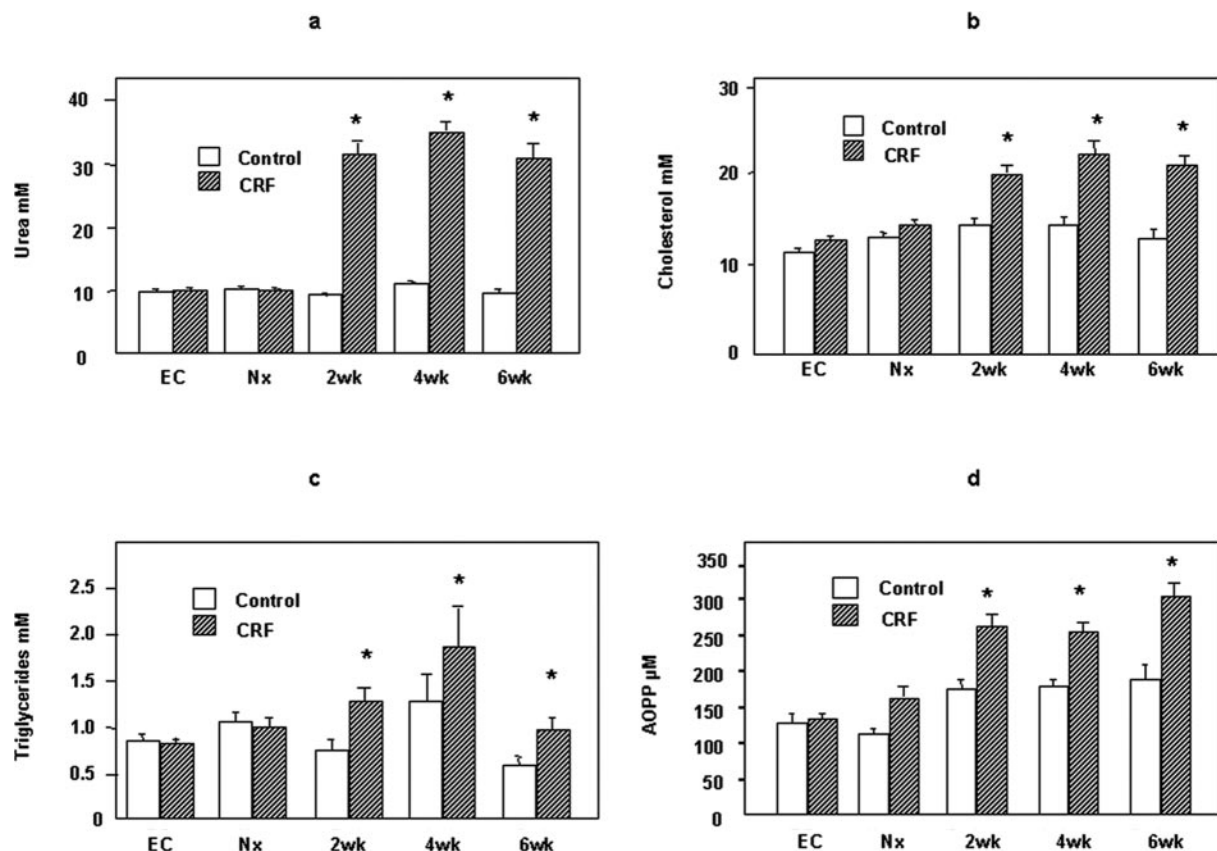


Figure 1. Serum concentrations of urea (A), total cholesterol (B), triglycerides (C), and advanced oxidation protein products (AOPP; D). Apolipoprotein E-deficient (apoE^{-/-}) mice were subjected to either sham operation (control mice) or a two-step creation of chronic renal failure (CRF). CRF mice, *n* = 22; control mice, *n* = 25. EC, electrocoagulation of right renal cortex; Nx, left total nephrectomy. *P* < 0.001 ANOVA between groups. **P* < 0.05 Fischer *post hoc* least significant difference test between control and CRF.

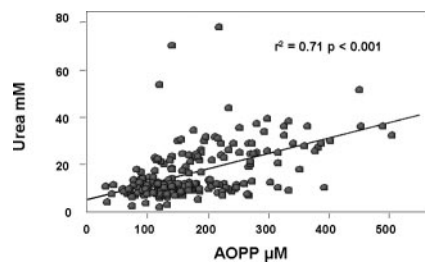


Figure 2. Correlation between serum AOPP and serum urea in the CRF and control apoE^{-/-} groups collapsed together. CRF mice, $n = 22$; control mice, $n = 25$.

($P < 0.04$; Figure 3). The impact of uremia on atherosclerosis in the aortic root seemed to be less pronounced because lesion sizes at this site were comparable in the two groups (Table 2). Also in the aortic root, lesions were larger and more advanced in female than in male apoE^{-/-} mice ($P = 0.03$; data not shown).

Aortic Calcification, Total Collagen Content, and MOMA Infiltration

CRF apoE^{-/-} mice had significantly larger areas of atheromatous and medial calcification than nonuremic apoE^{-/-} mice (Table 2, Figure 4). Moreover, intimal and medial calcification sizes were increased in CRF mice compared with controls, although this difference reached statistical significance only in the intima. There were no correlations between intimal or medial calcification area or size and serum calcium, phosphorus, calcium \times phosphorus product, cholesterol, triglycerides, AOPP, or atherosclerotic lesion area (data not shown). However, a significant correlation was observed in uremic mice between intimal and medial calcification area ($r^2 = 0.94$, $P < 0.001$) and between intimal and medial calcification sizes ($r^2 = 0.66$, $P < 0.001$), suggesting a link between atherosclerotic and medial vascular calcification.

FTIR spectroscopy confirmed a significant overall increase of mineral density in the plaques of CRF apoE^{-/-} mice compared with control mice. Moreover, it showed that the calcium deposits were made of hydroxyapatite (carapatite) and calcite (calcium carbonate anhydrous) crystals in both the intimal and

medial lesion sites. The calcium deposits in the intimal lesions were frequently co-localized with the presence of cholesterol crystals (Figure 5).

Finally, uremia was associated with a 38% increase in plaque collagen content (Table 2). However, the percentage of lesion cross-section area occupied by macrophages, as revealed by MOMA-2 staining, was comparable between the two groups (Table 2).

Discussion

The present findings lend support to the controversial view that the uremic state results in accelerated atherosclerosis. We found that 6 wk of CRF increased plaque progression in the thoracic aorta of CRF apoE^{-/-} mice compared with controls. This finding is in agreement with two other recent reports in uremic apoE^{-/-} mice (14,15) and extend the results by showing that CRF increased plaque progression as early as 6 wk of uremia duration. It is of interest that Bro *et al.* (23) recently reported lack of lesion formation in male uremic mice at 2 wk of uremia.

In addition to accelerated atherosclerosis, we found that CRF mice had significant increases in aortic vessel calcification. To the best of our knowledge, this is the first report of vascular calcification in the apoE^{-/-} model of atherosclerosis combined with CRF. The uremic state is associated with numerous metabolic abnormalities and endocrine disturbances, including abnormalities in calcium and phosphate metabolism and an inflammatory syndrome. These dysfunctions occur early in the course of CRF and contribute to the development and progression of vascular calcification and atherosclerosis. Severe calcifications of both the medial wall layer and the intima have been reported frequently in uremic patients (11,24). Although it is possible at present to quantify arterial calcifications in humans with electron-beam computed tomography or spiral computed tomography, these noninvasive techniques do not allow one to distinguish intima from media calcification and to study their respective progression. Animal studies provide the possibility of separately assessing the progression of vessel calcification at different anatomic sites to determine whether CRF differentially modifies the extent of intima and media calcification and

Table 1. Effect of CRF on MAP, serum urea, calcium, phosphorus, Ca \times P product, and iPTH in 16-wk-old apoE^{-/-} mice, 6 wk after creation of CRF^a

	Control Mice ($n = 24$)	CRF Mice ($n = 18$)	P
MAP (mmHg) ^b	69.7 \pm 2.1	72.8 \pm 3.4	NS
Urea (mM)	8.1 \pm 0.2	28.8 \pm 1.9	<0.0001
Calcium (mM)	2.28 \pm 0.22	2.55 \pm 0.03	<0.0001
Phosphate (mM)	1.94 \pm 0.71	2.15 \pm 0.72	<0.05
Ca \times P (mM ²)	4.4 \pm 0.1	5.4 \pm 0.2	<0.001
iPTH (pg/ml)	46 \pm 7	166 \pm 53	<0.05

^aValues are means \pm SEM. apoE^{-/-}, apolipoprotein E gene knockout; CRF, chronic renal failure; MAP, mean arterial BP; Ca \times P, calcium phosphorus product; iPTH, intact parathyroid hormone.

^b $n = 6$ and 6 for control and CRF mice, respectively.

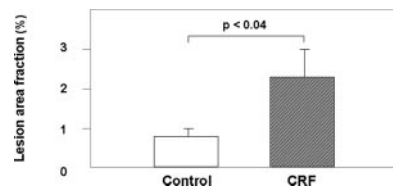


Figure 3. Atherosclerotic lesion cross-section area in thoracic aorta of control apoE^{-/-} and CRF apoE^{-/-} mice. CRF mice, *n* = 22; control mice, *n* = 25. Data are means ± SEM.

of testing new strategies aimed at arresting the progression or causing regression of vascular calcium deposits.

Enhanced medial calcification was observed previously in uremic rats (25) and rabbits (26). However, in addition to medial calcification, calcification of the intima was reported in only one recent study that examined CRF-induced atherosclerosis in the LDL receptor-deficient (LDLR^{-/-}) mouse (27). In this study, vessel wall calcification was evaluated only semi-quantitatively. In contrast, we were able for the first time to quantify calcium deposits in the intimal plaque area and media of aortic tissue by using a technique recently established in our laboratory (19). In both the intimal and medial layer of the aorta, we found a significant increase in calcified area in uremic mice compared with nonuremic controls. Surprising is that two recent reports that examined CRF in apoE^{-/-} mice (14,15) failed to observe calcification in the aortic wall despite a longer duration of uremia (12 and 22 wk, respectively). One possible explanation for this disparity is differences in the dietary regimen. Our diet contained a higher calcium/phosphate ratio (1.6) than those of the two previous studies (1.0 and 1.3 respectively), and this ratio has been shown to be an important factor for the regulation of intestinal calcium absorption (28). In addition, our dietary vitamin D₃ content (1540 IU/kg) was almost three times higher than in the previous work (600 IU/kg). In the present study, serum calcium, phosphorus, and iPTH concentrations were higher in CRF than in non-CRF apoE^{-/-} mice. All of these parameters are well-known factors that favor soft tissue calcification in patients with CRF. However, the degree of severity of calcium and phosphorus was comparable between our CRF apoE^{-/-} mice and those in the former two studies. It is possible that differences in dietary factors such as

relative amounts of protein, carbohydrate, and lipid, as well as their composition, may have contributed to the development of vascular calcification in our experimental model. However, we found that male CRF apoE^{-/-} mice had slower progression of vascular calcification than their female counterparts (data not shown). This could have contributed to the difference in vascular calcification between the present study and previous studies when male mice were used exclusively (14,15). Of note, sex differences of proteinuria (29), atheroma progression (30), and atheromatous lesion calcification (31) have also been reported in apoE^{-/-} mice with normal renal function.

To characterize further arterial calcification in apoE^{-/-} mice, we used FTIR spectroscopy and found that calcium deposits in both the intimal lesions and medial layers were made of hydroxyapatite and calcite crystals. Our data are in line with previous data in human coronary arteries in which calcified plaques of ESRD patients contained only hydroxyapatite and calcium phosphate but not calcium oxalate crystals (10). That calcification was increased in both the intima and the media is compatible with CRF-associated disturbances, leading to an increase in soft tissue calcification in general. Hyperphosphatemia may play an important role, in addition to hypercalcemia (32). However, a definitive conclusion about the respective roles of hyperphosphatemia and hypercalcemia in CRF apoE^{-/-} mice can be drawn only from an intervention designed to modify their levels separately and to measure subsequently changes in vascular calcification. Of note, a recent randomized clinical trial in dialysis patients showed prevention of the progression of vascular calcification by the non-calcium-containing binder sevelamer, in contrast to calcium-containing phosphate binders. However, there was no distinction between aortic and coronary artery localization in the media and the intima, respectively (33).

Additional factors other than excess calcium or phosphate likely participate in the pathogenesis of vascular calcification (34). The intimal lesions were frequently co-localized with cholesterol crystals. The increase in serum total cholesterol in CRF apoE^{-/-} mice compared with control mice may be such a factor contributing to accelerated atherosclerosis and vascular calcification (32).

Oxidative stress and inflammation have been recognized to

Table 2. Effect of CRF on plaque progression and composition in aortic root of 16-wk-old apoE^{-/-} mice, 6 wk after creation of CRF^a

	Control Mice (<i>n</i> = 25)	CRF Mice (<i>n</i> = 22)	<i>P</i>
Aortic root lesions (%)	19.6 ± 1.6	18.1 ± 1.3	NS
Macrophage infiltration (%)	12.5 ± 1.5	10.5 ± 2.1	NS
Collagen content (%)	12.5 ± 1.0	18.9 ± 2.3	0.012
Intima calcification area (%)	6.1 ± 0.03	17.8 ± 0.05	0.047
Intima calcification size (μm ²)	401 ± 67	817 ± 137	0.006
Media calcification area (%)	1.0 ± 0.01	3.8 ± 0.01	0.041
Media calcification size (μm ²)	340 ± 24	373 ± 26	NS

^aValues are means ± SEM.

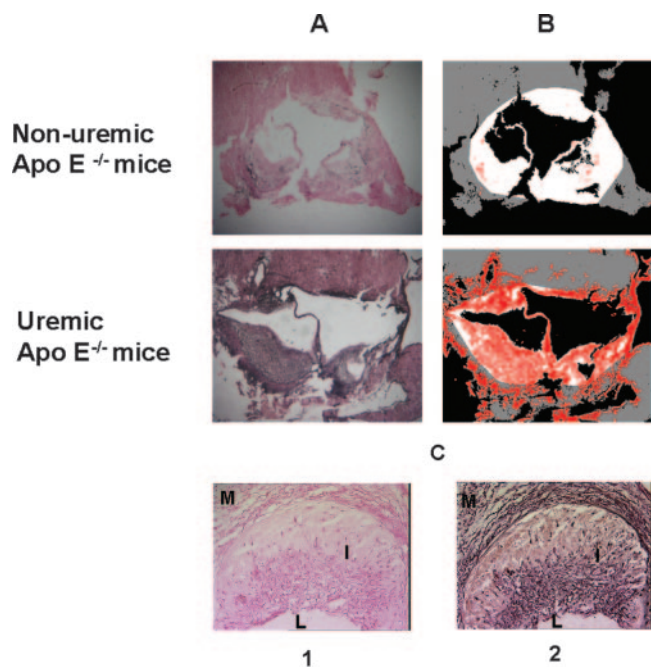


Figure 4. Representative images of aorta root sections of control apoE^{-/-} and CRF apoE^{-/-} mice. (A) Von Kossa silver nitrate staining (calcification in black). (B) Morphologic image processing (calcification in red) (C) Representative images of aortic root of CRF apoE^{-/-} mouse showing a higher magnification ($\times 10$) of the object after 2% eosin (1) as well as after 2% eosin and von Kossa staining (2). M, media; I, intima; L, lumen.

play a central role in the pathogenesis of cardiovascular disease in uremia (35). In the present study, CRF apoE^{-/-} mice had an increase in serum AOPP, which is a marker of chlorinated-oxidative stress. However, we did not find correlations between intimal or medial calcification area or size and AOPP. Buzello *et al.* (14) and Bro *et al.* (15) observed an increase in nitrotyrosine expression (a marker of nitrosative-oxidative stress) in the aortic wall of CRF apoE^{-/-} mice, although they did not report a correlation. This increase might point to the possible importance of nitrosative stress in the accelerated atherosclerosis of CRF apoE^{-/-} mice. In dialysis patients, however, chlorinated stress seems to prevail, because we and others did not observe an increase of plasma nitrotyrosine levels, whereas high concentrations of plasma chlorinated markers were present (36,37). Surprising is that a protective role for myeloperoxidase-generated reactive intermediates has been observed even in murine atherosclerosis (38), in agreement with possible difference between murine and human atherosclerosis development with regard to the involvement of chlorinated stress.

At present, there is only limited information on the impact of uremia on atherosclerotic plaque composition. In the present experimental setting, the atheromatous lesions of uremic animals exhibited a marked increase in collagen content as well as high calcite and hydroxyapatite content, although there was no evidence of increased infiltration by inflammatory cells. It remains unclear to which extent arterial wall inflammation con-

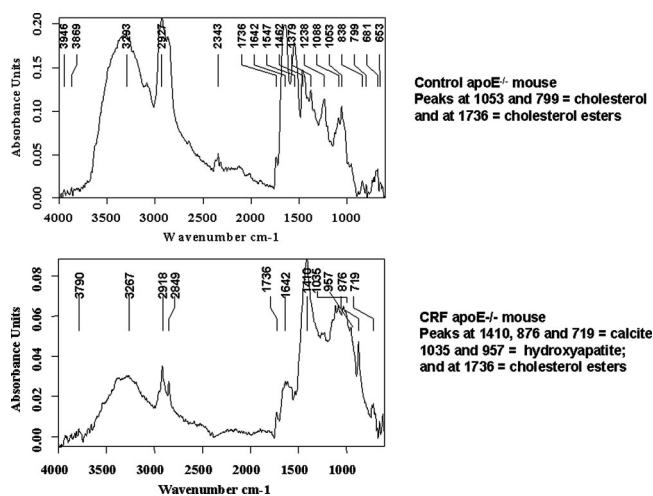


Figure 5. Fourier transformed infrared spectroscopy of aortic tissue of an apoE^{-/-} mouse with CRF and a control apoE^{-/-} mouse, respectively, showing an overall increase in mineral density (calcite and hydroxyapatite peaks) in the plaques of CRF apoE^{-/-} mice. Typical peaks of calcite are seen at 1410, 876, and 719 cm⁻¹, and those of hydroxyapatite at 1035 and 957 cm⁻¹, respectively.

tributes to the enhanced atherosclerosis and calcium deposition observed in the CRF apoE^{-/-} mice. It is interesting that a recent study in men (albeit not in women) failed to show a correlation between circulating C-reactive protein, a potent marker of inflammation, and coronary artery calcification, which is an index of atherosclerosis, suggesting that the widely accepted association between inflammation and atherosclerosis and/or calcification is more complex than was generally thought (39). However, C-reactive protein serum concentration was observed to be inversely related to that of fetuin-A (a negative acute-phase protein and an extracellular calcium regulatory molecule), and low fetuin-A concentrations in sera were found to be associated with enhanced all-cause and cardiovascular mortality in chronic hemodialysis patients (40). This complex relationship is currently under investigation in our laboratory. Obviously, other proteins with high calcium affinity such as bone matrix proteins also play an important role, both systemically and locally, in the determination of vascular calcium deposition (11,41). The observed accumulation of collagen in plaques might also have contributed.

At present, the excessive cardiovascular mortality in CRF patients continues to represent an unmet challenge. Various approaches to reduce premature atherosclerosis and vascular calcification in such patients will need to be tested to evaluate their efficacy and practicability. A major limiting factor in uremia-accelerated vascular calcification has been the lack of appropriate animal models. We propose that the CRF apoE^{-/-} mouse, in addition to the CRF LDLR^{-/-} mouse, provides a suitable model to analyze the different molecular and cellular mechanisms responsible for this serious complication of chronic kidney disease. Moreover, it may provide a useful tool for the evaluation of new therapeutic strategies aimed at reduc-

ing the accelerated atherosclerosis and vascular calcification associated with uremia.

Acknowledgments

O.I. was funded by a grant from Egide Foundation (Paris, France).

This study was presented as an abstract at the World Congress of Nephrology, June 8–12, 2003, Berlin, Germany.

We thank Nadine Bouby, PhD, Inserm Unit 367, Paris, for use of a BP recording device; Ziad Mallat, MD, PhD, INSERM Unit 541, Lariboisière Hospital (Paris, France) and Antonino Nicoletti, PhD, INSERM unit 430, Broussais Hospital (Paris, France), for expert technical advice.

References

- Foley RN, Parfrey PS, Sarnak MJ: Epidemiology of cardiovascular disease in chronic renal disease. *J Am Soc Nephrol* 9: S16–23, 1998
- London GM, Drueke TB: Atherosclerosis and arteriosclerosis in chronic renal failure. *Kidney Int* 51: 1678–1695, 1997
- Drueke T, Witko-Sarsat V, Massy Z, Descamps-Latscha B, Guerin AP, Marchais SJ, Gausson V, London GM: Iron therapy, advanced oxidation protein products, and carotid artery intima-media thickness in end-stage renal disease. *Circulation* 106: 2212–2217, 2002
- Kato A, Takita T, Maruyama Y, Kumagai H, Hishida A: Impact of carotid atherosclerosis on long-term mortality in chronic hemodialysis patients. *Kidney Int* 64: 1472–1479, 2003
- O'Hare AM, Glidden DV, Fox CS, Hsu CY: High prevalence of peripheral arterial disease in persons with renal insufficiency: Results from the National Health and Nutrition Examination Survey 1999–2000. *Circulation* 109: 320–323, 2004
- Stenvinkel P, Heimburger O, Paultre F, Diczfalusy U, Wang T, Berglund L, Jogestrand T: Strong association between malnutrition, inflammation, and atherosclerosis in chronic renal failure. *Kidney Int* 55: 1899–1911, 1999
- Wang AY, Wang M, Woo J, Lam CW, Li PK, Lui SF, Sanderson JE: Cardiac valve calcification as an important predictor for all-cause mortality and cardiovascular mortality in long-term peritoneal dialysis patients: a prospective study. *J Am Soc Nephrol* 14: 159–168, 2003
- Blacher J, Guerin AP, Pannier B, Marchais SJ, London GM: Arterial calcifications, arterial stiffness, and cardiovascular risk in end-stage renal disease. *Hypertension* 38: 938–942, 2001
- Raggi P, Boulay A, Chasan-Taber S, Amin N, Dillon M, Burke SK, Chertow GM: Cardiac calcification in adult hemodialysis patients. A link between end-stage renal disease and cardiovascular disease? *J Am Coll Cardiol* 39: 695–701, 2002
- Schwarz U, Buzello M, Ritz E, Stein G, Raabe G, Wiest G, Mall G, Amann K: Morphology of coronary atherosclerotic lesions in patients with end-stage renal failure. *Nephrol Dial Transplant* 15: 218–223, 2000
- Moe SM, O'Neill KD, Duan D, Ahmed S, Chen NX, Leapman SB, Fineberg N, Kopecky K: Medial artery calcification in ESRD patients is associated with deposition of bone matrix proteins. *Kidney Int* 61: 638–647, 2002
- Guerin AP, London GM, Marchais SJ, Metivier F: Arterial stiffening and vascular calcifications in end-stage renal disease. *Nephrol Dial Transplant* 15: 1014–1021, 2000
- Muntzel MMZ, Ruellan N, Descamps-Latscha B, Lacour B, Drueke TB: Chronic renal failure increases oxidative stress and accelerates atherosclerosis in apolipoprotein-E knockout (EKO) mice [Abstract]. *Nephrol Dial Transplant* 17[Suppl 1]: 46, 2002
- Buzello M, Tornig J, Faulhaber J, Ehmke H, Ritz E, Amann K: The apolipoprotein e knockout mouse: A model documenting accelerated atherogenesis in uremia. *J Am Soc Nephrol* 14: 311–316, 2003
- Bro S, Bentzon JF, Falk E, Andersen CB, Olgaard K, Nielsen LB: Chronic renal failure accelerates atherogenesis in apolipoprotein e-deficient mice. *J Am Soc Nephrol* 14: 2466–2474, 2003
- Plump AS, Smith JD, Hayek T, Aalto-Setälä K, Walsh A, Verstuyft JG, Rubin EM, Breslow JL: Severe hypercholesterolemia and atherosclerosis in apolipoprotein E-deficient mice created by homologous recombination in ES cells. *Cell* 71: 343–353, 1992
- Gagnon RF, Gallimore B: Characterization of a mouse model of chronic uremia. *Urol Res* 16: 119–126, 1988
- Witko-Sarsat V, Friedlander M, Capeillere-Blandin C, Nguyen-Khoa T, Nguyen AT, Zingraff J, Jungers P, Descamps-Latscha B: Advanced oxidation protein products as a novel marker of oxidative stress in uremia. *Kidney Int* 49: 1304–1313, 1996
- Angulo J, Nguyen-Khoa T, Massy ZA, Drueke TB, Serra J: Morphological quantification of aortic calcification from low magnification images. *Image Anal Stereol* 22: 81–89, 2003
- Dao NG, Daudon M: *Infrared and Raman Spectra of Calculi*, Paris, Elsevier, 1997
- Mallat Z, Gojova A, Marchiol-Fournigault C, Esposito B, Kamate C, Merval R, Fradelizi D, Tedgui A: Inhibition of transforming growth factor-beta signaling accelerates atherosclerosis and induces an unstable plaque phenotype in mice. *Circ Res* 89: 930–934, 2001
- Meneton P, Ichikawa I, Inagami T, Schnermann J: Renal physiology of the mouse. *Am J Physiol Renal Physiol* 278: F339–F351, 2000
- Bro S, Moeller F, Andersen CB, Olgaard K, Nielsen LB: Increased expression of adhesion molecules in uremic atherosclerosis in apolipoprotein-E-deficient mice. *J Am Soc Nephrol* 15: 1495–1503, 2004
- Ibels LS, Alfrey AC, Huffer WE, Craswell PW, Anderson JT, Weil R 3rd: Arterial calcification and pathology in uremic patients undergoing dialysis. *Am J Med* 66: 790–796, 1979
- Ejerblad S, Eriksson I, Johansson H: Uraemic arterial disease. An experimental study with special reference to the effect of parathyroidectomy. *Scand J Urol Nephrol* 13: 161–169, 1979
- Tvedegaard E: Arterial disease in chronic renal failure—an experimental study in the rabbit. *Acta Pathol Microbiol Immunol Scand Suppl* 290: 1–28, 1987
- Davies MR, Lund RJ, Hruska KA: BMP-7 is an efficacious treatment of vascular calcification in a murine model of atherosclerosis and chronic renal failure. *J Am Soc Nephrol* 14: 1559–1567, 2003
- Masuyama R, Nakaya Y, Katsumata S, Kajita Y, Uehara M, Tanaka S, Sakai A, Kato S, Nakamura T, Suzuki K: Dietary

- calcium and phosphorus ratio regulates bone mineralization and turnover in vitamin D receptor knockout mice by affecting intestinal calcium and phosphorus absorption. *J Bone Miner Res* 18: 1217–1226, 2003
29. Ivanovski O, Nguyen-Khoa T, Phan O, Massy ZA: Could proteinuria evaluation be helpful in predicting renal progression in apolipoprotein E-deficient (E^{-/-}) mice with chronic renal failure? *Nephrol Dial Transplant* 19: 1013–1014; author reply 1014, 2004
 30. Caligiuri G, Nicoletti A, Zhou X, Tornberg I, Hansson GK: Effects of sex and age on atherosclerosis and autoimmunity in apoE-deficient mice. *Atherosclerosis* 145: 301–308, 1999
 31. Qiao JH, Xie PZ, Fishbein MC, Kreuzer J, Drake TA, Demer LL, Lusis AJ: Pathology of atheromatous lesions in inbred and genetically engineered mice. Genetic determination of arterial calcification. *Arterioscler Thromb* 14: 1480–1497, 1994
 32. Moe SM, Chen NX: Pathophysiology of vascular calcification in chronic kidney disease. *Circ Res* 95: 560–567, 2004
 33. Chertow GM, Burke SK, Raggi P: Sevelamer attenuates the progression of coronary and aortic calcification in hemodialysis patients. *Kidney Int* 62: 245–252, 2002
 34. Moe SM, Duan D, Doehle BP, O'Neill KD, Chen NX: Uremia induces the osteoblast differentiation factor Cbfa1 in human blood vessels. *Kidney Int* 63: 1003–1011, 2003
 35. Himmelfarb J, Stenvinkel P, Ikizler TA, Hakim RM: The elephant in uremia: Oxidant stress as a unifying concept of cardiovascular disease in uremia. *Kidney Int* 62: 1524–1538, 2002
 36. Massy ZA, Borderie D, Nguyen-Khoa T, Drueke TB, Ekindjian OG, Lacour B: Increased plasma S-nitrosothiol levels in chronic haemodialysis patients. *Nephrol Dial Transplant* 18: 153–157, 2003
 37. Himmelfarb J, McMennamin ME, Loseto G, Heinecke JW: Myeloperoxidase-catalyzed 3-chlorotyrosine formation in dialysis patients. *Free Radic Biol Med* 31: 1163–1169, 2001
 38. Brennan ML, Anderson MM, Shih DM, Qu XD, Wang X, Mehta AC, Lim LL, Shi W, Hazen SL, Jacob JS, Crowley JR, Heinecke JW, Lusis AJ: Increased atherosclerosis in myeloperoxidase-deficient mice. *J Clin Invest* 107: 419–430, 2001
 39. Reilly MP, Wolfe ML, Localio AR, Rader DJ: C-reactive protein and coronary artery calcification: The Study of Inherited Risk of Coronary Atherosclerosis (SIRCA). *Arterioscler Thromb Vasc Biol* 23: 1851–1856, 2003
 40. Ketteler M, Bongartz P, Westenfeld R, Ernst Wildberger J, Horst Mahnken A, Bohm R, Metzger T, Wanner C, Jahnke-Dechent W, Floege J: Association of low fetuin-A (AHSG) concentrations in serum with cardiovascular mortality in patients on dialysis: A cross-sectional study. *Lancet* 361: 827–833, 2003
 41. Shanahan CM, Proudfoot D, Tyson KL, Cary NR, Edmonds M, Weissberg PL: Expression of mineralisation-regulating proteins in association with human vascular calcification. *Z Kardiol* 89[Suppl 2]: 63–68, 2000